Synthesis and electrical conductivity of nanocrystalline tetragonal FeS*

Zeng Shu-Lin(曾树林)[a)b)], Wang Hui-Xian(王辉宪)[a)], and Dong Cheng(董 成)[b)†]

[a)] *Hunan Agricultural University, Changsha* 410128, *China*

[b)] *Beijing National Laboratory for Condensed Matter Physics, Institute of Physics, Chinese Academy of Sciences, Beijing* 100190, *China*

(Received 25 April 2014; revised manuscript received 29 May 2014; published online 20 June 2014)

A convenient method for synthesis of tetragonal FeS using iron powder as iron source, is reported. Nanocrystalline tetragonal FeS samples were successfully synthesized by reacting metallic iron powder with sodium sulfide in acetate buffer solution. The obtained sample is single-phase tetragonal FeS with lattice parameters $a = 0.3767$ nm and $c = 0.5037$ nm, as revealed by X-ray diffraction. The sample consists of flat nanosheets with lateral dimensions from 20 nm up to 200 nm and average thickness of about 20 nm. We found that tetragonal FeS is a fairly good conductor from the electrical resistivity measurement on a pellet of the nanosheets. The temperature dependence of conductivity of the pellet was well fitted using an empirical equation wherein the effect of different grain boundaries was taken into consideration. This study provides a convenient, economic way to synthesize tetragonal FeS in a large scale and reports the first electrical conductivity data for tetragonal FeS down to liquid helium temperature.

Keywords: tetragonal FeS, synthesis method, electrical conductivity, grain boundary

PACS: 72.15.Eb, 73.63.Bd, 81.07.Bc, 81.20.Ka **DOI:** 10.1088/1674-1056/23/8/087203

1. Introduction

Tetragonal FeS has attracted increasing attention because it has a layered structure, fascinating properties, and important potential applications. It crystallizes in a tetragonal anti-PbO structure ($P4/nmm$ space group), which is composed of layers of edge-sharing FeS_4 tetrahedra.[1,2] Mackinawite is a naturally occurring tetragonal FeS mineral, important in biogeochemical cycles.[3] Synthetic tetragonal FeS has been explored as a photocathode in solar cells[4] and as a material for microbial fuel cells.[5] It is known to be an effective scavenger for metal pollutants[6–8] and a strong reducing reagent for chromate and chlorinated organic compounds.[9–11] The possibility of superconductivity in tetragonal FeS has attracted much interest because it is isostructural to the FeSe superconductor[12] and exhibits the magnetic characteristics of the Fe-based superconductors.[13–16] Kwon *et al.* reported spectroscopic evidence and density functional theory calculations supporting the existence of strong itinerant spin fluctuations in tetragonal FeS in 2011.[16] They conjectured that tetragonal FeS may be one of the simplest Fe-based superconductors if strong spin fluctuations are the mediators of electron pairing.

The lack of single-crystal samples of tetragonal FeS has limited attempts to define its electrical and magnetic properties.[17] Very limited data can be found in the literature on electrical conductivity of tetragonal FeS. To the best of our knowledge, the only report was given by Bertaut *et al.* in 1965.[18] They measured the resistance of tetragonal FeS obtained by reacting metallic iron with H_2S solution, and found that the resistance decreases linearly from 12.5 Ω/cm to 2 Ω/cm as temperature increases from 80 K to 300 K. Mössbauer spectroscopy indicates that tetragonal FeS has no magnetic ordering down to 4.2 K.[19] In order to test the possible superconductivity of tetragonal FeS by resistivity measurements down to liquid helium temperature, it is necessary to prepare well-crystallized tetragonal FeS.

Tetragonal FeS is a metastable phase and highly reactive to oxygen in air,[3,20] so it is difficult to prepare pure and well-crystallized samples. Tetragonal FeS transforms into other more stable phases, such as greigite (Fe_3S_4),[21] pyrrhotite ($Fe_{1-x}S$, $0 < x < 0.2$),[22] and pyrite (FeS_2),[23,24] depending on temperature, time courses, and redox conditions. Tetragonal FeS is easily oxidized by O_2 in air to form magnetite (Fe_3O_4).[20] The direct synthesis of tetragonal FeS from elemental Fe and S has not been achieved.[1] Two common ways for synthesizing tetragonal FeS are used in the literature; they involve either the precipitation of aqueous ferrous ions Fe^{2+}[3,25] or the reaction of metallic iron[1,25] with a dissolved sulfide solution. Poorly-crystallined tetragonal FeS can be formed in cultures of certain bacteria.[26] In addition, tetragonal FeS films can be deposited by electrochemical methods.[27,28] The reaction of metallic iron with aqueous sulfide usually results in a better crystalline product than other methods.[29–32] Iron wires are often used as the iron source in literature because the unreacted iron wires can be easily re-

*Project supported by the National Natural Science Foundation of China (Grant No. 21271183) and the National Basic Research Program of China (Grant Nos. 2011CBA00112 and 2011CB808202).

†Corresponding author. E-mail: chengdon@aphy.iphy.ac.cn

© 2014 Chinese Physical Society and IOP Publishing Ltd

moved. Unreacted iron remained in the product after 6 days reaction when iron powder was used as the reactant.[25] A new solvothermal crystallization method was reported in 2012[33] to synthesize tetragonal FeS nanosheets with high crystallinity. However, a serious problem to be solved is that the product made by the solvothermal crystallization method contains impurities. To eliminate the impurities in tetragonal FeS produced by the solvothermal crystallization, we tried several experimental conditions but failed.

In this study tetragonal FeS samples were synthesized by the reaction of iron powder with sulfide solution. Iron powder was chosen as iron source material since fine and pure iron wires are very expensive. In order to separate unreacted iron powder from the product, we utilized a magnet in the experiment. Pure and well-crystallized tetragonal FeS samples were successfully synthesized by reacting iron powder with sulfide solution, because unreacted iron powder, stuck to the magnet, could be separated easily from the product. The tetragonal FeS samples were characterized by X-ray powder diffraction (XRD), scanning electron microscopy (SEM), and electrical resistivity measurements.

2. Experimental section

Iron powder (-200 mesh, $\geq 99\%$) was purchased from Alfa Aesar. Acetic acid ($\geq 99.0\%$), sodium acetate ($\geq 99.0\%$), ferrous chloride ($FeCl_2{\cdot}4H_2O$, $\geq 99.0\%$), and sodium sulfide ($Na_2S{\cdot}9H_2O$) were purchased from Sinapharm. All chemicals were of analytical grade and were used without further purification.

Tetragonal FeS is very sensitive to oxygen, so special care is needed to prevent oxidation during synthesis and subsequent process. All solutions were prepared with deaerated deionized water, deaerated with N_2 bubbling for at least 30 minutes. Moreover, the preparation of test samples was conducted in a glovebox filled with high-purity argon.

Firstly, 0.5-M HAc–NaAc buffer solution (pH = 4.9) and 0.45-M Na_2S solution were prepared. 500-ml buffer solution was added into a beaker. A magnet (with a diameter of 5 cm and a thickness of 0.5 cm) was used to separate the product tetragonal FeS from unreacted iron powder. The magnet was put into a zip-lock plastic bag to prevent it from reacting with the solution. Then iron powder (4 g) was placed near the bag so that it sticks to the exterior surface of the bag around the magnet. The plastic bag was hung on a glass rod with support of the beaker, immersing the iron powder in the buffer solution. To prevent air from entering the solution, the beaker was covered with aluminum foil, and n-hexane (~ 5 ml) was added on the top of the buffer solution. Bubbles of hydrogen gas began to appear soon after the iron powder was immersed in the acetate buffer. Figure 1 shows the experimental setups before the addition of the Na_2S solution.

After 3.5 h, 50-ml Na_2S solution was injected slowly, and the pH value changed to approximately 5.3. Black flocculent precipitates formed instantly and settled slowly to the bottom of the beaker. This solution, containing the iron powder, was allowed to stand at room temperature for 24 hours.

The plastic bag along with the unreacted iron powder was then removed from the beaker vessel and the supernatant was discarded. The obtained precipitation was washed with deaerated and deionized water and centrifuged three times at 4000 r/min. The product was dried subsequently at 50 °C for 2 h under vacuum. The powder sample was sealed in a vial and kept in a glovebox for subsequent analyses.

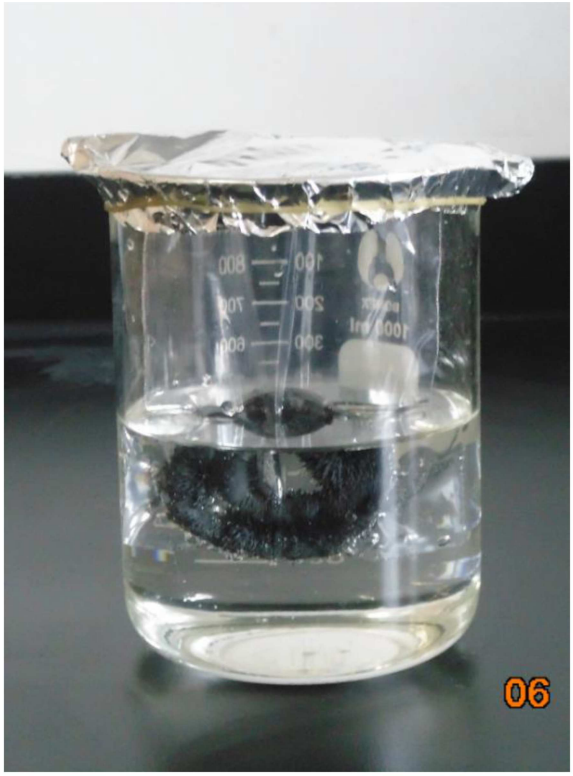


Fig. 1. The experimental setup for the synthesis of tetragonal FeS.

Powder X-ray diffraction data were collected on a Rigaku Ultima-IV X-ray diffractometer using Cu K_α radiation. Phase identification was conducted using the Jade-6.0 (MDI, United States) computer program and the lattice parameters were refined using the least-square method with the PowderX program.[34]

The morphology of the sample was observed by an XL30 S-FEG scanning electron microscope. Tetragonal FeS cannot be sintered since it transforms to hexagonal pyrrhotite (FeS) above 160 °C.[18] We had to make the electrical resistivity measurement using a pelletized sample. The tetragonal FeS powder obtained above was pressed into a pellet 10 mm in diameter and 1-mm thick under the pressure of 10 MPa. The measured density of the pellet sample is 2.9 g/cm^3. The elec-

trical resistivity measurement was performed using a standard four-probe method between 5 K and 300 K.

3. Results and discussion

Pure and well-crystallized tetragonal FeS samples were obtained by the reaction of iron powder with sulfide solution. Figure 2 shows the powder X-ray diffraction (XRD) pattern for the tetragonal FeS product. No impurity peak is observed in the diffraction pattern, and all peaks can be indexed to the tetragonal FeS phase with lattice parameters $a = 0.3767(1)$ nm, $c = 0.5037(1)$ nm, close to that reported in the literature.[1] The SEM micrographs of the tetragonal FeS (Fig. 3) show that it consists of flat nanosheets. The lateral dimensions of the nanosheets are 20 nm up to 200 nm and the average thickness is about 20 nm. Almost all crystallites have the same flat-sheet morphology, indicating high phase purity of the tetragonal FeS sample. Therefore, only the samples synthesized by this method were used in subsequent measurements of electrical properties.

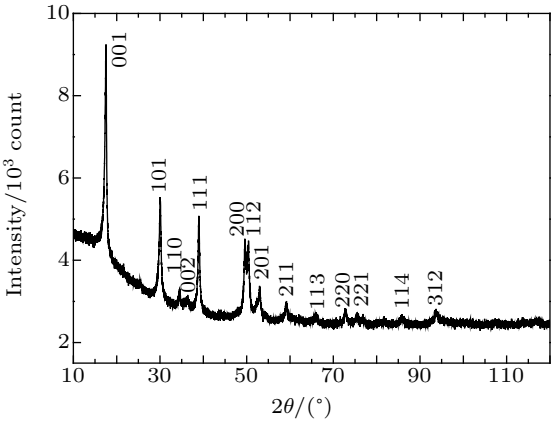


Fig. 2. Powder XRD pattern of tetragonal FeS obtained by reaction of iron powder with sulfide solution.

The resistivity versus temperature curve, obtained from measurements of the pelletized nanosheets, is plotted in Fig. 4. From the resistivity measurements, we found that the sample is a fairly good conductor because its resistivity at room temperature (298 K) is only 48 μΩ·cm, much lower than that of polycrystalline graphite (300 μΩ·cm–6000 μΩ·cm)[35] and even less than the in-plane resistivity of single-crystal graphite (55 μΩ·cm–65 μΩ·cm).[36] Such a low resistivity in our pelletized nanosheets indicates that bulk tetragonal FeS is most likely a metal, at least in the *ab* plane, in agreement with the prediction by first-principles calculations.[14–16] However, the resistivity ρ increases linearly as temperature decreases from 300 K to 100 K, so the temperature coefficient of resistivity is negative. Within this temperature range, ρ can be well fitted (with the adjusted *R*-square = 0.99965) by a linear relation, $\rho = 72.32 - 0.08494T$ (μΩ·cm), where T is the temperature in unit K. Below 100 K, the resistivity deviates from linear dependence and increases more quickly with decreasing temperature, and this could be attributed to the effect of grain boundaries.

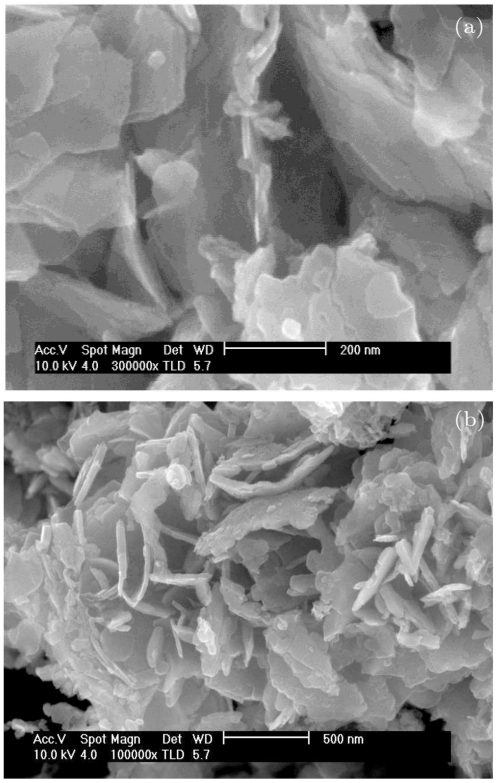


Fig. 3. Representative SEM images of the tetragonal FeS nanosheets with high magnification (a) and low magnification (b).

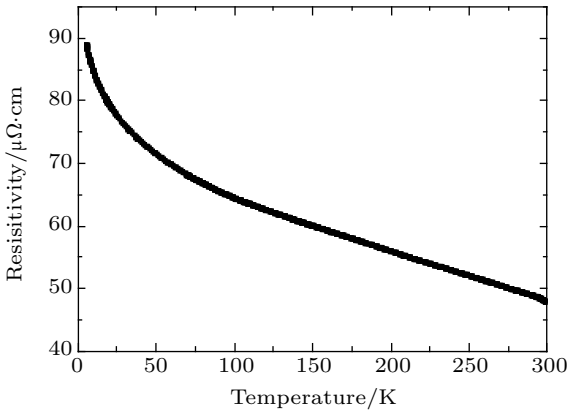


Fig. 4. Temperature dependence of the resistivity for pelletized tetragonal FeS nanosheets.

Since the nanosheets have different sizes and orientations, their grain boundaries are expected to distribute inhomogeneously and constitute an intricate network. The measured density of the pellet used for the electrical measurement is about 2.9 g/cm^3, which is only two-thirds of the density (4.29 g/cm^3) calculated from the crystal structure of tetragonal FeS. Consequently, microscopic voids occupy about one-third of sample volume, and the grain boundaries will dominate the temperature dependence of conductivity. We tried

several models to fit the conductivity ($\sigma = \rho^{-1}$) versus temperature curve, and found that the curve, seemingly smooth, could not be fitted well by a simple equation in the form of $\sigma = \sigma_0 \exp(-CT^{-\alpha})$, where σ_0 and C are fitting parameters, and α was set as 1, 1/2, and 1/4 respectively, three different α values corresponding to three electrical conduction mechanisms, 1 to the thermally activated process,[37] 1/2 to granular metal,[38] and 1/4 to variable range hopping.[39] Three Arrhenius plots $\ln(\sigma)$ versus $T^{-\alpha}$ ($\alpha = 1, 1/2, 1/4$) were drawn and all three plots are curved. A typical Arrhenius plot of resistivity as a function of temperature is shown in Fig. 5.

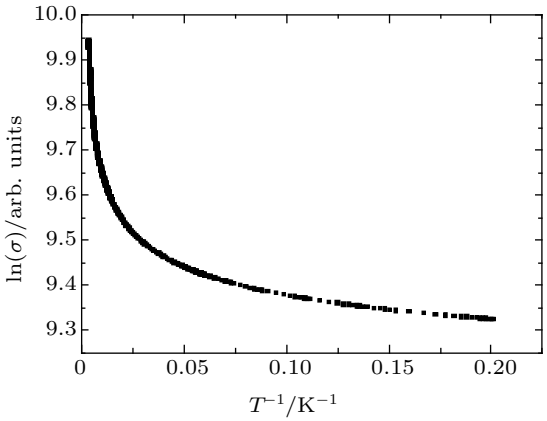


Fig. 5. Arrhenius plot of resistivity as a function of temperature for the tetragonal FeS sample.

The origin of the curved Arrhenius plot, as explained by Werner,[40] is spatial potential fluctuations of inhomogeneous grain boundaries. The spatial potential fluctuations give rise to temperature-dependent activation energy E_a. Assuming the spatial potential fluctuation can be modeled by a Gaussian distribution, it can be derived that the activation energy E_a varies linearly with T^{-1}.[40] However, the derivative $\partial \ln(\sigma/\mathrm{T})/\partial T^{-1}$ versus T^{-1} plot is also not linear for the tetragonal FeS sample, so the activation energy does not vary linearly with T^{-1}. This can be attributed to severe inhomogeneity of the grain boundaries. Since the electrical conduction of the grain boundaries is essentially a thermally activated process, the activation energies can be determined from the slope of the curve in the Arrhenius plot (Fig. 5). The slope of the curve, i.e. the activation energy, changes more than two orders of magnitude from 5 K to 298 K. For that reason, we designed an empirical equation to fit the conductivity data,

$$\sigma(T) = \sigma_0 + C_{\mathrm{H}} \exp(-E_{\mathrm{H}}/k_{\mathrm{B}}T) + C_{\mathrm{M}} \exp(-E_{\mathrm{M}}/k_{\mathrm{B}}T) + C_{\mathrm{L}} \exp(-E_{\mathrm{L}}/k_{\mathrm{B}}T), \quad (1)$$

where σ_0 is the temperature-independent conductivity, E_{H}, E_{M}, and E_{L} are the high, medium, and low activation energies in that order, C_{H}, C_{M}, and C_{L} are pre-exponential factors, and k_{B} is the Boltzmann constant. The physical meaning of σ_0 is the conductivity from the grains in close contact, and other terms are the conductivity from grain boundaries with representative high, medium, and low potential barrier heights. The temperature dependence of conductivity of the tetragonal FeS was fitted excellently ($R = 0.99997$) using the empirical equation. Figure 6 shows the experimental and the fitting results, and Table 1 lists the obtained parameters in Eq. (1).

From Table 1, we can see that the σ_0 is quite large. This result suggests that bulk tetragonal FeS is probably a metal, because the temperature-independent term σ_0 corresponds to a zero slope in the Arrhenius plot, i.e., a zero activation energy. No signal of superconducting transition was observed in the conductivity data from 300 K down to 5 K.

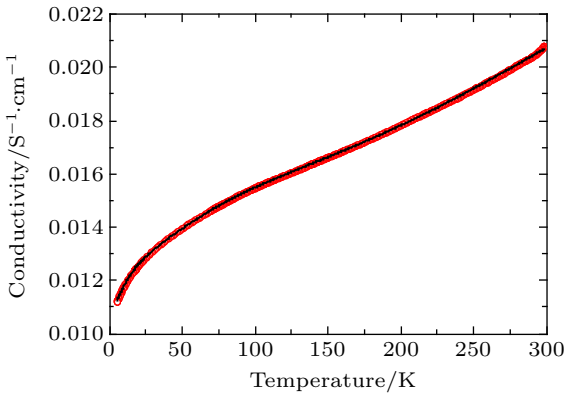


Fig. 6. (color online) Temperature dependence of conductivity of the tetragonal FeS. Small circles represent experimental data, and the solid line represents the fitting results using Eq. (1).

Table 1. Parameters in Eq. (1) obtained by fitting the experimental conductivity data.

σ_0/S^{-1}·cm^{-1}	C_{L}/S^{-1}·cm^{-1}	C_{M}/S^{-1}·cm^{-1}	C_{H}/S^{-1}·cm^{-1}	E_{L}/meV	E_{M}/meV	E_{H}/meV
0.011125	0.003208	0.005441	0.043063	1.33	10.5	69.3

4. Conclusions

In order to study the physical properties, especially possible superconductivity, of tetragonal FeS, pure and well-crystallined tetragonal FeS nanosheets were successfully obtained by reactions of iron powder with sulfide solutions, and characterized by powder X-ray diffraction and scanning electron microscopy. This method is very economical and suitable to large scale preparation of tetragonal FeS, because iron powder is much cheaper than previously used high-purity fine iron wires.

The electrical conductivity measurements of a tetragonal-FeS pellet show that it is a fairly good conductor, and the temperature dependence of conductivity was well fitted using an empirical equation. This empirical equation has potential applications in fitting conductivity data of similar nanomaterials. Based on the experimental conductivity data, we infer that

bulk tetragonal FeS is probably a metal. Although no sign of superconducting transition of the tetragonal FeS nanosheets was observed, it might be possible to introduce superconductivity by elemental doping and substitution, similar to the success with FeSe.[41]

References

[1] Lennie A R, Redfern S A T, Schofield P F and Vaughan D J 1995 *Mineral Mag.* **59** 677
[2] Uda M 1968 *Z. Anorg. Allg. Chem.* **361** 94
[3] Rickard D and Luther G W 2007 *Chem. Rev.* **107** 514
[4] Hu Y, Zheng Z, Jia H M, Tang Y W and Zhang L Z 2008 *J. Phys. Chem. C* **112** 13037
[5] Nakamura R, Okamoto A, Tajima N, Newton G J, Kai F, Takashima T and Hashimoto K 2010 *Chembiochem* **11** 643
[6] Farquhar M L, Charnock J M, Livens F R and Vaughan D J 2002 *Environ. Sci. Technol.* **36** 1757
[7] Jeong H Y, Klaue B, Blum J D and Hayes K F 2007 *Environ. Sci. Technol.* **41** 7699
[8] Watson J H P, Cressey B A, Roberts A P, Ellwood D C, Charnock J M and Soper A K 2000 *J. Magn. Magn. Mater.* **214** 13
[9] Patterson R R, Fendorf S and Fendorf M 1997 *Environ. Sci. Technol.* **31** 2039-44
[10] Jeong H Y and Hayes K F 2007 *Environ. Sci. Technol.* **41** 6390
[11] Jeong H Y, Kim H and Hayes K F 2007 *Environ. Sci. Technol.* **41** 7736
[12] Hsu F C, Luo J Y, Yeh K W, Chen T K, Huang T W, Wu P M, Lee Y C, Huang Y L, Chu Y Y, Yan D C and Wu M K 2008 *Proc. Natl. Acad. Sci. USA* **105** 14262
[13] Wilson J A 2010 *J. Phys.: Condens. Matter* **22** 203201
[14] Devey A J, Grau-Crespo R and De Leeuw N H 2008 *J. Phys. Chem. C* **112** 10960
[15] Subedi A, Zhang L J, Singh D J and Du M H 2008 *Phys. Rev. B* **78** 134514
[16] Kwon K D, Refson K, Bone S, Qiao R M, Yang W L, Liu Z and Sposito G 2011 *Phys. Rev. B* **83** 064402
[17] Pearce C I, Pattrick R A D and Vaughan D J 2006 *Rev. Mineral Geochem.* **61** 127
[18] Bertaut E F, Burlet P and Chappert J 1965 *Solid State Commun.* **3** 335
[19] Vaughan D J and Ridout M S 1971 *J. Inorg. Nucl. Chem.* **33** 741
[20] Boursiquot S, Mullet M, Abdelmoula M, Genin J M and Ehrhardt J J 2001 *Phys. Chem. Miner.* **28** 600
[21] Lennie A R, Redfern S A T, Champness P E, Stoddart C P, Schofield P F and Vaughan D J 1997 *Am. Mineral* **82** 302
[22] Lennie A R, England K E R and Vaughan D J 1995 *Am. Mineral* **80** 960
[23] Hunger S and Benning L G 2007 *Geochem. Trans.* **8** 1
[24] Wilkin R T and Barnes H L 1996 *Geochim. Cosmochim. Acta* **60** 4167
[25] Berner R A 1964 *Journal of Geology* **72** 293
[26] Gramp J P, Bigham J M, Jones F S and Tuovinen O H 2010 *J. Hazard Mater.* **175** 1062
[27] Bezdicka P, Grenier J C, Fournes L, Wattiaux A and Hagenmuller P 1989 *Eur. J. Solid State Inorg. Chem.* **26** 353
[28] Gomes A, Pereira M I D, Mendonca M H and Costa F M 2002 *Solid State Sci.* **4** 1083
[29] Mullet M, Boursiquot S, Abdelmoula M, Genin J M and Ehrhardt J J 2002 *Geochim. Cosmochim. Acta* **66** 829
[30] Wolthers M, Van Der Gaast S J and Rickard D 2003 *Am. Mineral* **88** 2007
[31] Csakberenyi-Malasics D, Rodriguez-Blanco J D, Kis V K, Recnik A, Benning L G and Posfai M 2012 *Chem. Geol.* **294** 249
[32] Ohfuji H and Rickard D 2006 *Earth Planet. Sci. Lett.* **241** 227
[33] Sines I T, Vaughn D D, Misra R, Popczun E J and Schaak R E 2012 *J. Solid State Chem.* **196** 17
[34] Dong C 1999 *J. Appl. Crystallogr.* **32** 838
[35] Kaye G W C and Laby T H 1995 *Tables of Physical and Chemical Constants* (Beijing: Longman) p. 152
[36] Edman L, Sundqvist B, Mcrae E and Litvin-Staszewska E 1998 *Phys. Rev. B* **57** 6227
[37] Efros A and Shklovskii B 1984 *Springer Series in Solid-State Sciences* (Berlin: Springer) **45** pp. 74–93
[38] Sheng P, Abeles B and Arie Y 1973 *Phys. Rev. Lett.* **31** 44
[39] Mott N 1969 *Philos. Mag.* **19** 835
[40] Werner J 1994 *Solid State Phenom.* **37** 213
[41] Guo J, Jin S, Wang G, Wang S, Zhu K, Zhou T, He M and Chen X 2010 *Phys. Rev. B* **82** 180520